Toxicology in Vitro 73 (2021) 105112

Contents lists available at ScienceDirect

Toxicology in Vitro

journal homepage: www.elsevier.com/locate/toxinvit

Evaluation of a human iPSC-derived BBB model for repeated dose toxicity testing with cyclosporine A as model compound

Sara Wellens [a], Lucie Dehouck [a], Vidya Chandrasekaran [b], Pranika Singh [c,d], Rodrigo Azevedo Loiola [a], Emmanuel Sevin [a], Thomas Exner [c], Paul Jennings [b], Fabien Gosselet [a], Maxime Culot [a,*]

[a] University of Artois, UR 2465, Laboratoire de la Barrière Hémato-Encéphalique (LBHE), Faculté des sciences Jean Perrin, Rue Jean Souvraz SP18, F-62300 Lens, France

[b] Division of Molecular and Computational Toxicology, Department of Chemistry and Pharmaceutical Sciences, Amsterdam Institute for Molecules, Medicines and Systems, Vrije Universiteit Amsterdam, De Boelelaan 1108, 1081HZ Amsterdam, the Netherlands

[c] Edelweiss Connect GmbH, Technology Park Basel, Hochbergerstrasse 60C, 4057 Basel, Switzerland

[d] Division of Molecular and Systems Toxicology, Department of Pharmaceutical Sciences, University of Basel, Klingelbergstrasse 50, 4056 Basel, Switzerland

ARTICLE INFO

Keywords:
iPSC
Blood-brain barrier
Repeated dose toxicity testing
Targeted transcriptomics
Cyclosporine A
Stress-response pathways

ABSTRACT

The blood-brain barrier (BBB) is a highly restrictive barrier that preserves central nervous system homeostasis and ensures optimal brain functioning. Using BBB cell assays makes it possible to investigate whether a compound is likely to compromise BBBs functionality, thereby probably resulting in neurotoxicity. Recently, several protocols to obtain human brain-like endothelial cells (BLECs) from induced pluripotent stem cells (iPSCs) have been reported. Within the framework of the European MSCA-ITN in3 project, we explored the possibility to use an iPSC-derived BBB model to assess the effects of repeated dose treatment with chemicals, using Cyclosporine A (CsA) as a model compound. The BLECs were found to exhibit important BBB characteristics up to 15 days after the end of the differentiation and could be used to assess the effects of repeated dose treatment. Although BLECs were still undergoing transcriptional changes over time, a targeted transcriptome analysis (TempO-Seq) indicated a time and concentration dependent activation of ATF4, XBP1, Nrf2 and p53 stress response pathways under CsA treatment. Taken together, these results demonstrate that this iPSC-derived BBB model and iPSC-derived models in general hold great potential to study the effects of repeated dose exposure with chemicals, allowing personalized and patient-specific studies in the future.

1. Introduction

Neurotoxicity assessment of chemicals is essential for their safety evaluation. Current neurotoxicity testing for regulatory purposes, following OECD guidelines, is still based on resource intensive animal studies (Bal-Price et al., 2018). Nevertheless, there is an ongoing movement towards the use of non-animal test methods for neurotoxicity and developmental neurotoxicity (Bal-Price et al., 2018; Fritsche, 2017; Sirenko et al., 2019). Many of these test methods make use of human induced pluripotent stem cells (iPSCs) derived neural cultures containing neuronal and glial cells, allowing better toxicity prediction by use of human cells. However, neurotoxicity assessment of chemicals does not solely rely on their interaction with brain cells but also on their ability to reach these cells by crossing the blood-brain barrier (BBB) (Schultz et al., 2015). This selective barrier is composed of specialized endothelial cells at the level of the brain capillaries that contain physical components (i.e. tight-junctions), metabolic components (i.e. metabolizing enzymes) and transport processes (i.e. presence of efflux transporters (e.g. ABCB1 and ABCG2) and solute carrier transporters (e.g. SLC2A1)) in conjunction with perivascular elements (such as closely

Abbreviations: BBB, Blood-Brain Barrier; BLECs, Brain-Like Endothelial Cells; BMECs, Brain Microvascular Endothelial Cells; CLDN5, Claudin 5; CsA, Cyclosporine A; DOT, Day Of Treatment; EC, Endothelial Cell; HUVEC, Human Umbilical Vein Endothelial Cell; INT, p-iodonitrotetrazolium violet; iPSC, induced Pluripotent Stem Cell; NGS, Normal Goat Serum; PBS-CMF, Phosphate Buffered Saline–Calcium Magnesium Free; Rho123, Rhodamine 123; RH, HEPES-buffered Ringer's solution; RT, Room Temperature; TEER, Transendothelial Electrical Resistance; VE-cadherin, Vascular Endothelial Cadherin.

* Corresponding author.
E-mail address: maxime.culot@univ-artois.fr (M. Culot).

https://doi.org/10.1016/j.tiv.2021.105112
Received 1 December 2020; Received in revised form 25 January 2021; Accepted 9 February 2021
Available online 22 February 2021
0887-2333/© 2021 The Authors. Published by Elsevier Ltd. This is an open access article under the CC BY-NC-ND license (http://creativecommons.org/licenses/by-nc-nd/4.0/).

associated pericytes, astrocyte end-feet processes and perivascular neurons). Altogether, the functions of the BBB endothelium maintain brain homeostasis. Therefore, interaction of chemicals with the BBB can lead to neurotoxicity by jeopardizing the barrier integrity and creating a homeostatic disturbance of the brain. Multiple human *in vitro* BBB models have been developed, starting with scarce primary cells and followed by immortalized cell lines (like hCMEC/D3, hBMEC, TY10 and BB19) (Eigenmann et al., 2013). More recently, BBB models have been derived from hematopoietic stem cell (Cecchelli et al., 2014) and endothelial progenitor cell-based BBB co-culture models (Boyer-Di Ponio et al., 2014) or human induced pluripotent stem cells (iPSCs) (Workman and Svendsen, 2020) to overcome some of the challenges faced with immortalized cell lines like the low paracellular barrier properties (Weksler et al., 2005). As pericytes and astrocytes play an important role in the development and maintenance of the BBB (Obermeier et al., 2013), some of these protocols make use of these perivascular cells in the differentiation process to induce a BBB phenotype (with a decrease in permeability and upregulation of BBB genes) (Appelt-Menzel et al., 2017; Canfield et al., 2019; Canfield et al., 2017; Cecchelli et al., 2014). The availability of unlimitedly self-renewing human iPSCs, which could be differentiated in all cell types with the same genetic background, allows the development of isogenic neurovascular unit models (Canfield et al., 2019; Canfield et al., 2017) and has opened new opportunities for the evaluation of chemical toxicity (Logan et al., 2019).

Within the framework of the in3 project (Marie Sklodowska-Curie Action-Innovative Training Network 2017–2020 grant no. 721975, www.estiv.org/in3), we intended to explore the possibility to use iPSCs for chemical toxicity assessment by differentiating iPSCs into specific cell types: neural, lung, liver, kidney (Rauch et al., 2018) and vasculature lineages including BBB and exposing it to various compounds.

In the recent years, several protocols have been published to differentiate iPSCs into brain-like endothelial cells (BLECs) (Appelt-Menzel et al., 2017; Canfield et al., 2019; Canfield et al., 2017; Hollmann et al., 2017; Lippmann et al., 2014; Lippmann et al., 2013) but the possibility to use these models for repeated dose toxicity testing has not yet been explored. Among these iPSC differentiation protocols to BLECs, Qian *et al.* reported at the end of 2017 a completely chemically defined method using a developmentally pertinent progression by activation of Wnt and retinoic acid pathway using small-molecule activation (Qian et al., 2017). As this protocol enables to avoid the use of serum which batch-to-batch variation affects the barrier properties of brain microvascular endothelial cells (Neal et al., 2019), the chemically defined protocol reported by Qian *et al.* has been used in this study.

In order to study the effects of repeated dose treatment, the immunosuppressive drug Cyclosporine A (CsA) has been used, which is extensively prescribed to prevent graft rejection after transplantation. However, its use often leads to nephrotoxicity and sometimes to hepatotoxicity and neurotoxicity (Hauben, 1996; Wu et al., 2018). Given its reported chronic side effects, the molecular mechanism of CsA toxicity has been studied in different cell types using Chip-Seq data and transcriptomics (Limonciel et al., 2015, 2018; Wilmes et al., 2011), demonstrating the activation of different stress response pathways (like ATF4, XBP1 and Nrf2). Therefore, we selected CsA as a model compound and investigated the stress response pathways activated by repeated dose treatment with CsA on BLECs derived from iPSCs.

The objectives of this study were (i) to investigate the long-term stability of the iPSC differentiated BLECs and (ii) to evaluate the possibility to use such model for repeated dose toxicity testing using CsA.

2. Materials and methods

2.1. Cell culture (iPSC differentiation protocol)

The SBAD3 clone 1 iPSC cell line, already used by several members of the in3 project, was obtained from the Innovative Medicines Initiative-funded StemBANCC consortium (grant agreement no 115439, http://stembancc.org) and maintained as described in Rauch *et al.* (Rauch et al., 2018). iPSCs were differentiated into BLECs according to the protocol of Qian *et al.* with minor modifications (Qian et al., 2017). Briefly, undifferentiated iPSCs were first passaged with Accutase (#07920, Stemcell technologies) as small colonies and plated at a density of 20.8 k cells/cm^2 on Matrigel-coated (83 μg/mL, 354230, Corning) 6 well plates (3506, Corning) in mTeSR (#85850, Stemcell technologies) with 10 μM Rho kinase inhibitor Y-27632 (stock concentration: 5 mM in DMSO; Ab120-129, Abcam). The day after, the medium was changed to DeSR1 (DMEM/F12 (HEPES) (11330–032, Thermo Fisher Scientific) with 1× MEM non-essential amino acids (11140–050, Thermo Fisher Scientific), 0.5× Glutamax (35050–061, Thermo Fisher Scientific) and 0.1 mM β-Mercaptoethanol (M3148, Sigma)) supplemented with 6 μM CHIR99021 (stock concentration: 3 mM in DMSO; SML1046, Sigma) for 24 h. Subsequently the cells were kept in DeSR2 (DMEM/F12 (HEPES) with 1× MEM non-essential amino acids, 0.5× Glutamax, 0.1 mM β-Mercaptoethanol and 1× B27 supplement (17504044, Thermo Fisher Scientific)) for three or four days with a medium change every 24 h. Then, the cells were changed to hECSR1 (human endothelial serum-free medium (11111-044, Thermo Fisher Scientific) with 20 ng/mL basic fibroblast growth factor (stock: dissolved in Tris (1 mg/mL) and diluted in DMEM with 0.1% bovine serum albumin (100 μg/mL); 100-18B, Peprotech), 10 μM all-trans retinoic acid (stock concentration: 5 mM in DMSO; R2625, Sigma) and 1× B27) for 48 h, passaged with Accutase and seeded in hECSR1 medium at a density of 1 million cells/cm^2 on Matrigel-coated (100 μg/mL) 96 well plates (161093, Thermo Fisher Scientific) or transwell inserts with 0.4 μm pore size (3401, Corning). One day after the passage, the medium was changed to hECSR2 (human endothelial serum-free medium with 1× B27, without bFGF and RA) and this was continued every 48 h until the end of the protocol.

2.2. Transendothelial electrical resistance (TEER)

The resistance of the seeded or coated inserts was measured, using the EVOM2 device (with chopstick, World precision instruments), immediately after the inserts were taken out of the incubator. If a medium change needed to be performed on the same day, this was done after the resistance measurement. For the calculation of the TEER, the resistance of the coated inserts without cells was subtracted from the resistance with cells and multiplied by the surface area of the insert (1.12 cm^2). TEER measurements were performed on triplicates of inserts of two independent differentiations.

2.3. Functionality of efflux transporters

The functionality of efflux transporters was assessed, at day of treatment (DOT) 0 and DOT 14, by comparing the rate of clearance of the fluorescent efflux transporter substrate, rhodamine 123 out of the cells (Rho123 K_{out}) in the presence or absence of the competitive inhibitors elacridar and verapamil as described by Sevin *et al.* (Sevin et al., 2019). Elacridar, rhodamine 123 (Rho123) and verapamil were obtained from Sigma-Aldrich (Saint Quentin Fallavier, France) and were first dissolved in DMSO to achieve stock concentrations which enable dilution to their final concentration in buffer while reducing the DMSO concentration to 0.1%.

The cells (8 replicates/condition), seeded in 96-well plates, were washed once with HEPES-buffered Ringer's (RH) solution (NaCl 150 mM, KCl 5.2 mM, $CaCl_2$ 2.2 mM, $MgCl_2$ 0.2 mM, $NaHCO_3$ 6 mM, Glucose 2.8 mM, HEPES 5 mM, water for injection), pH = 7.4 before incubation with 10 μM Rho123, dissolved in RH, for 120 min. After rinsing, the cells were incubated with elacridar (final concentration = 20 μM), verapamil (final concentration = 50 μM) or without any compound (0.1% DMSO) in RH for one hour at 37 °C during which Rho123 (λ_{ex} = 485 nm and λ_{em} = 538 nm) was measured using a microplate fluorescence reader (Fluoroskan Ascent FL, Thermo Labsystems, Issy-Les-Moulineaux, France)

every 2 min. The slope of the cumulative Rho123 fluorescence curve against the time served to calculate the Rho123 K_{out}.

2.4. Immunocytochemistry

Cells cultivated on transwell inserts were fixed with ice-cold methanol (100%) for 10 min on ice. After washing three times with PBS-CMF (Phosphate Buffered Saline–Calcium Magnesium Free), sea block buffer (37527, Thermo Fisher Scientific) was added for 30 min, at room temperature (RT). Primary antibodies were diluted in PBS-CMF containing 2% normal goat serum (NGS, G-6767, Sigma) at following dilutions: Claudin 5 (34–1600, Invitrogen) 1/100 and VE-cadherin (ab33168, Abcam) 1/400. Following 1-h incubation at RT with the primary antibody, the filters were washed three times with 2% NGS (in PBS-CMF) and incubated with the secondary antibody (A11036, Invitrogen, 1/500 in PBS-CMF) for 30 min, at RT. After three rinses with PBS-CMF, inserts were mounted with Prolong Diamond Antifading Mountant containing DAPI (P36962, Invitrogen) on to glass slips. Samples were imaged using the confocal Operetta CLS high content imager (Perkin Elmer) with 63× water objective and the images were collected using Harmony software 4.9.

2.5. Cyclosporine A treatment regimen and cytotoxicity assessment (lactate and resazurin)

First, CsA (CAS: 59865–13-3, 30024, Sigma) was dissolved in DMSO and afterwards diluted thousand times in hECSR2 to the final concentrations (resulting in 0.1% DMSO in the cell assays). For repeated dose exposure, treatment of BLECs was initiated at DOT 0 and renewed every 48 h by refreshing medium containing either 5 μM CsA, 15 μM CsA or 0.1% DMSO (Fig. 1a).

The quantification of lactate in cell culture medium was performed using a corrected protocol based on Limonciel *et al.* (Limonciel et al., 2011). Supernatant medium samples for lactate measurement were taken at DOT 1, 3, 5, 11 and 15 from three independent wells of 96 well plates of two independent differentiations. For 7 min, 10 μL of supernatant medium was incubated with 90 μL of the lactate assay mix, composed of 86 mM triethanolamine HCl (T9534), 8.6 mM EDTA.Na (E4884), 34 mM $MgCl_2.6H_20$ (M8266), 326 μM N-Methylphenazonium methyl sulphate (PMS, P9625), 790 μM p-iodonitrotetrazolium violet

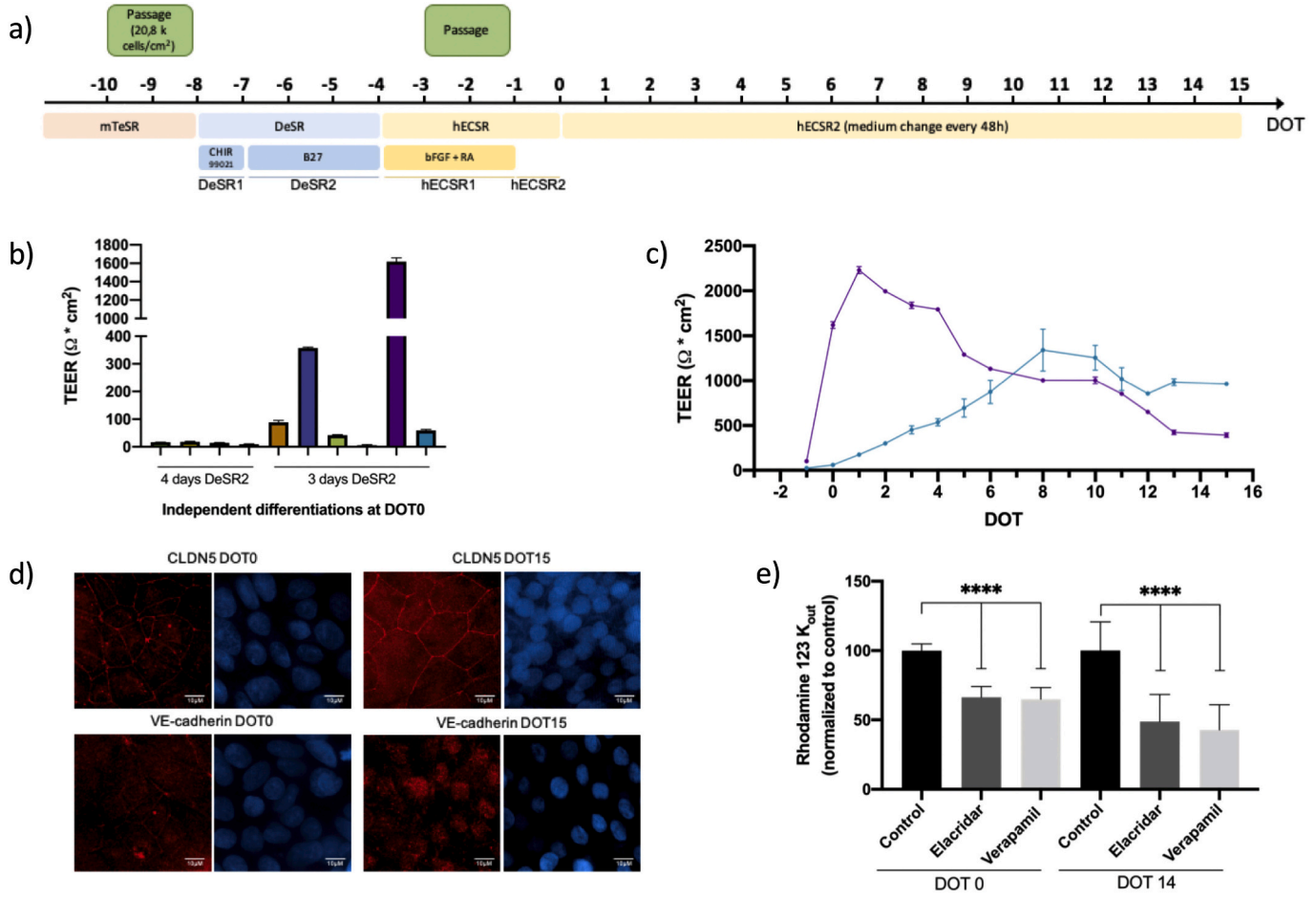


Fig. 1. iPSC-derived brain-like endothelial cells differentiation and subsequent 15 days culture.
a) Schematic of experimental protocol: first, iPSCs were differentiated into BLECs (day −12 to day 0) and then hECSR2 medium was changed every two days from DOT 0 till DOT 15.
b) Transendothelial Electrical Resistance (TEER) measured at DOT 0 after differentiation of iPSCs in DeSR2 medium for either 3 or 4 days. Values represent the mean ± SEM of three biological replicates for each independent differentiation.
c) TEER were measured daily from DOT 0 till DOT 15. Values represent the mean ± SEM of three biological replicates for two independent differentiations.
d) Immunostainings of differentiated BLECs at DOT 0 and DOT 15 for claudin 5 (CLDN5) or vascular endothelial cadherin (VE-cadherin). Cell nuclei were stained with DAPI. Scale bars represent 10 μm.
e) Rate of Rhodamine 123 (Rho123) clearance out of the differentiated BLECs at DOT 0 and DOT 14 in the presence and absence of elacridar (20 μM) or verapamil (50 μM). Values represent the mean ± SD of eight biological replicates for each condition. Statistical significance was determined using a two-way ANOVA with Sidak's multiple comparison test (****$p < 0.0001$).

(INT, I8377), 7% ethanol, 0.4% Triton-X-100 (X100), 3.3 mM β-Nicotinamide adenine dinucleotide (β-NAD, N7004) and 4 U/mL lactate dehydrogenase (LDH, L2500). All components were acquired from Sigma. Subsequently, the absorption of the reduced INT (to INTH) was measured using a microplate reader (Synergy H1, BioTek, Colmar, France) at 490 nm. The lactate concentrations of the unknown values were extrapolated from the standard lactate values using a spline fit function (using GraphPad Prism version 8.4.3).

The resazurin assay was performed as described by Jennings *et al.* (Jennings et al., 2007) on triplicates of two independent differentiations. A resazurin stock solution at 880 μM (R7017, Sigma) was prepared by first dissolving the powder in 0,1 N NaOH (0.011 g/mL) and subsequently diluted in PBS with a final pH of 7.8. BLECs in 96 well plates, were incubated with 44 μM resazurin in hECSR2 medium (100 μL/well) for 2 h. Fluorescence of the resazurin reduction product, resorufin, was measured with excitation at 540 nm and emission at 590 nm using the Synergy H1 plate reader.

2.6. TempO-Seq preparation and analysis

Duplicate wells of two independent differentiations in 96 well plates at time points DOT 0, 1, 3, 5, 11 and 15 were used for the targeted transcriptome quantification assay, TempO-Seq from BioSpyder (www.biospyder.com) (Yeakley et al., 2017). Cells were rinsed once with 200 μL sterile PBS-CMF and lysed using 160 μL 1× TempO-Seq lysis buffer per well. After 15 min incubation at room temperature, lysates were frozen and stored at −80 °C before shipment to BioClavis (Glasgow, UK) where the TempO-Seq assay was conducted. For TempO-Seq analysis, the 3565 probe-set representing 3257 genes were quantified (Table S1) following the same procedure as Limonciel *et al.* 2018 (Limonciel et al., 2018). FASTQ file from each sample was aligned against the TempO-Seq transcriptome using the Bowtie aligner (Li and Durbin, 2009). The output of this analysis generated a table of counts per gene per sample, further analysis was performed in R (script files S4). Assessment of outliers was done by the use of a correlation heatmap. No outliers were identified. The DESeq2 package was used for normalisation (Table S2), using the estimateSizeFactors function, and differentially expression analysis (Love et al., 2014). Differential expression analysis was performed of the treatment samples with their suitable control. Genes were considered significantly differentially expressed when the Benjamin Hochberg adjusted *p*-values were ≦ 0.05. For the generation of the Volcano plots with ggplot shrinkage of the log2 fold changes was applied.

Toxicity pathway analysis was performed using a list of genes annotated to different stress response pathways (for a complete list of pathway allocations see Table S1). These gene lists were used to calculate the z-score of the stress response pathways using the following formula (Kutmon et al., 2015) with N representing the total number of genes measured in the experiment, n the total number of genes of a certain pathway measured in the experiment, R the total number of genes with adjusted *p*-value <0.05 and r the number of genes with adjusted *p*-value <0.05 belonging to the pathway investigated. A *Z*-score above 1.96 or below −1.96 is considered significant.

$$Z - Score = \frac{\left(r - n\frac{R}{N}\right)}{\sqrt{n\left(\frac{R}{N}\right)\left(1 - \frac{R}{N}\right)\left(1 - \frac{n-1}{N-1}\right)}}$$

2.7. Statistical analysis

Statistical analysis was performed using GraphPad Prism version 8.4.3. One-way ANOVA with Sidak's multiple comparison test was used for the rate of rhodamine excretion graph (Fig. 1e). One-way ANOVA with Dunnett's multiple comparisons test was used for analysis of the resazurin assay performed at DOT 7 (Fig. 3c). Two-way ANOVA with Dunnett's multiple comparison test was used for analysis of the TEER measurements of the treated BLECs (Fig. 3a) and analysis of the lactate assay (Fig. 3b).

3. Results

3.1. iPSC-derived BBB model for repeated dose toxicity testing

Within the framework of this study, different protocols to differentiate iPSCs into BLECs have been explored and resulting iPSC derived-BLECs cultures have been evaluated for their ability to display some of the main characteristics of BBB-ECs such as restrictive tight junctions resulting in a high TEER and functional expression of efflux transporters (data not shown) (Hollmann et al., 2017; Lippmann et al., 2014; Qian et al., 2017). For two of these protocols (Hollmann et al., 2017; Lippmann et al., 2014) challenges were faced in reproducing the protocol as the platelet-poor plasma derived bovine serum was banned in the country of experimentation and the functional expression of efflux transporters could not be identified. Consequently, the directed differentiation protocol from Qian *et al.* (Qian et al., 2017) was selected and optimised for the SBAD3 clone 1 iPSC cell line (*Fig. 1*a). To evaluate the utility of the model for repeated dose toxicity testing, the BLECs were maintained for 15 days after the end of the differentiation protocol (day of treatment (DOT) 0 to DOT 15). At DOT 0, the restrictive permeability was assessed by TEER measurement to evaluate the differentiation (*Fig. 1*b). Differentiations of iPSCs resulting in a TEER lower than 25 Ω.cm^2 at DOT 0 were considered unsuccessful and excluded. Keeping these differentiations in culture for a longer time period did not result in an increase in the TEER (data not shown). To reproduce the original differentiation protocol as much as possible, multiple differentiation attempts were made with four days of DeSR2 medium. As this did not result in an increased TEER at DOT 0, the time in DeSR2 was shortened to three days. Although an increased TEER at DOT 0 was then frequently achieved, the variability between independent differentiations remained distinct (e.g. among successful differentiations the difference between the highest and lowest TEER at DOT 0 was more than 27-fold (1619 Ω.cm^2 and 59 Ω.cm^2 respectively). Two of these differentiations (most on the right in Fig. 1b) were kept for 15 days during which TEER was measured (*Fig. 1*c). One differentiation showed an immediate increase in TEER while for the other differentiation the maximum was achieved at DOT 8. At DOT 15, the lowest TEER was still 390 Ω.cm^2 which indicate that the BLECs still formed a restrictive barrier. This was also indicated by the immunostainings of the tight junction protein claudin 5 (CLDN5) which showed marginal membrane localization both at DOT 0 and DOT 15 (*Fig. 1*d). While the CLDN5 staining remained localized at the cell border after 15 days, the vascular endothelial cadherin (VE-cadherin) staining changed from a membrane localization at DOT 0 to an intracellular staining at DOT 15. The functionality of efflux transporters was evaluated by comparing the efflux clearance of the P-gp (ABCB1) and BCRP (ABCG2) (Alqawi et al., 2004; Özvegy et al., 2002) fluorescent substrate, Rhodamine 123 (Rho123), in the presence or absence of the inhibitors verapamil and elacridar (*Fig. 1*e). Both at DOT 0 and DOT 14, the reduced Rho123 K_{out} in the presence of inhibitors indicate the presence of functional efflux transporters. Taken as a whole, these data demonstrate that BLECs displayed some of the main features of BBB endothelial cells: high TEER, presence of VE-cadherin and tight junction protein CLDN5 and functional efflux transporter up to at least two weeks after differentiation and appears suitable for repeated dose toxicity testing.

3.2. Cyclosporine A concentration determination by acute toxicity assessment

The immunosuppressive drug CsA was selected to evaluate the effects of repeated dose-treatment on BLECs derived from iPSCs as the

molecular mechanisms of its nephro- and hepatotoxicity have been extensively studied whereas its effects at the BBB are still to be examined. We aimed to investigate the effects of repeated exposure of CsA at concentrations where no major cellular perturbations are observed after acute (24 h) treatment. Therefore, we first assessed the cytotoxicity of 24-h exposure of BLECs to CsA concentrations ranging from 1 μM to 20 μM using a resazurin assay (Fig. 2a). The amount of reduced resazurin (resorufin) signal was significantly lower at 20 μM CsA compared to the control. The similar redox capacity of BLECs following 24 h of treatment with CsA indicated the absence of cytotoxicity of the compounds for concentrations up to 15 μM. As 5 μM and 15 μM, so called therapeutic and supratherapeutic concentrations, were previously used to explore the effects of repeated dose exposure with CsA on human renal proximal tubule cells line (RPTEC/TERT1) (Wilmes et al., 2013) and these concentrations did not indicate any acute toxicity, these concentrations were selected for repeated dose exposure of BLECs to CsA (medium change every 48 h).

3.3. Cyclosporine A repeated dose toxicity assessment

TEER and lactate production were monitored throughout the experiment as parameters of cell-barrier tightness and cellular stress, respectively (Fabulas-da Costa et al., 2013; Limonciel et al., 2011). Additionally, cell viability was measured after 7 days of treatment with resazurin assay and samples were harvested for targeted RNA sequencing (TempO-Seq) at DOT 0, 1, 3, 5, 11 and 15 (Fig. 2b). Although, no effect of CsA treatment at either 5 μM and 15 μM on TEER was noted after one day of treatment (i.e DOT 1), the TEER of the BLECs cultures treated with both concentrations dropped from DOT 2 and remained lower than the control condition until DOT 15 (with a significantly lower TEER under treatment compared to control for both individual differentiations after DOT 5) (Fig. 3a). These results demonstrate a progressive loss of barrier tightness in BLECs culture treated with CsA resulting in absolute TEER below 100 Ω.cm^2 at both concentrations after DOT 12.

Various stress situations, like hypoxia, tissue repair, oxidative stress and mitochondrial dysfunction, can lead to an increase in lactate production via anaerobic metabolization of glucose (Limonciel et al., 2011). Therefore, enhanced lactate production may be considered as a global marker of sub-lethal injury. As lactate can be measured non-invasive in the supernatant medium, this is suitable marker for temporal monitoring during repeated dose toxicity testing. The significant higher amount of lactate, found in supernatant medium, 24 h after the onset of CsA treatment indicates increased cellular stress (*Fig. 3*b). Under 5 μM CsA treatment, the lactate production remained elevated compared to the untreated condition throughout the experiment (although not significantly at DOT 15). Under 15 μM CsA treatment, the lactate production was also elevated compared to the untreated condition from DOT 1 to DOT 11. However, the lactate production under 15 μM CsA was found unexpectedly lower compared to the 5 μM condition at DOT 3, 5 and 11 whereas a higher CsA concentration was expected to produce an at least similar cell stress. This can be explained by a reduction of cell viability

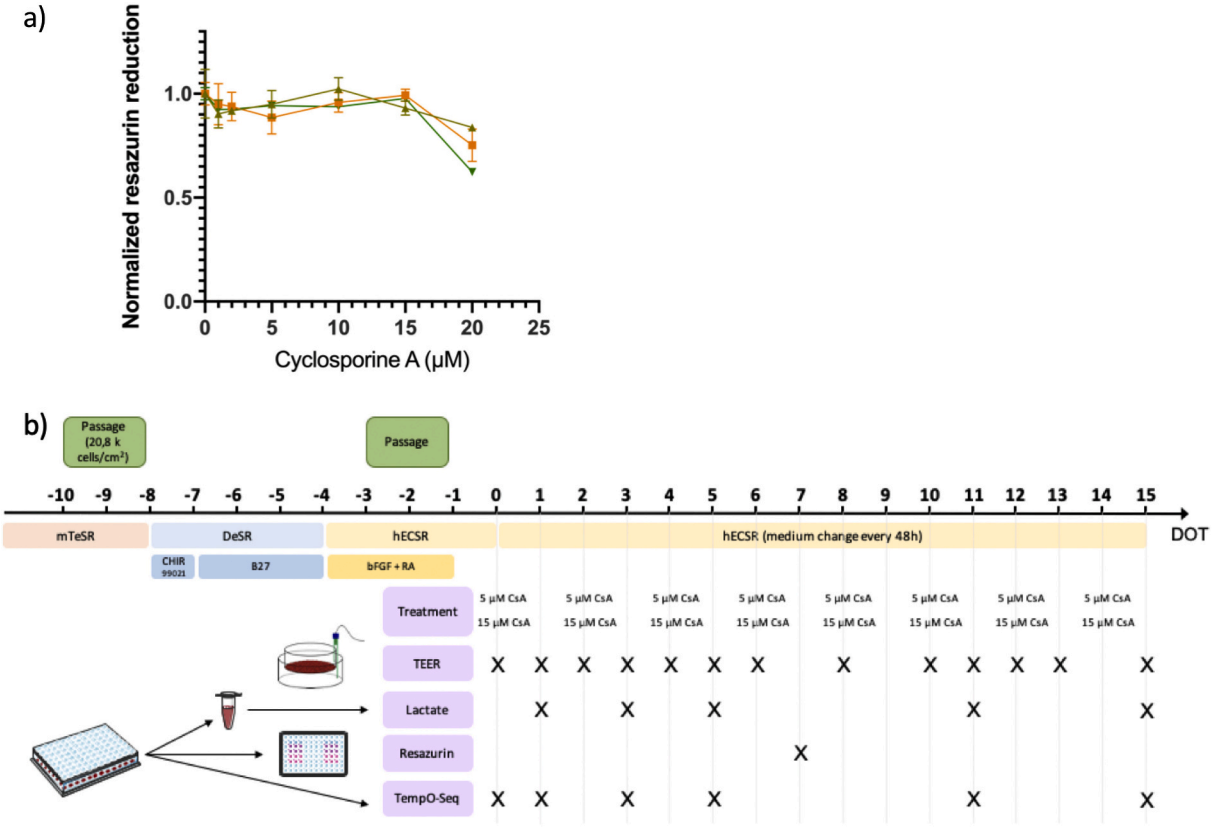


Fig. 2. Concentration determination and experimental outline for repeated dose toxicity testing.
a) Viability measurements in 96 well plates after 24 h of exposure to Cyclosporine A (CsA). iPSCs were differentiated into BLECs before initiating treatment with CsA. Resazurin assay was conducted after 24 h of treatment. Values represent the mean ± SD from three to six biological replicate for each independent differentiation normalized to resorufin reduction in the absence of CsA (with 0.1% DMSO).
b) Scheme of experimental procedure and sample generation. iPSCs differentiated into BLECs were cultivated either in 96-well plates or on permeable inserts and treatment with 5 μM or 15 μM CsA was initiated at DOT 0. Medium and treatment were renewed every 48 h from DOT 0 until DOT 15. TEER measurement and resazurin assays were performed at the indicated days. Samples for targeted RNA sequencing using TempO-Seq and lactate were harvested at set intervals as indicated.
Bottom left figures were modified from Servier Medical Art, licensed under a Creative Common Attribution 3.0 Generic License. http://smart.servier.com/

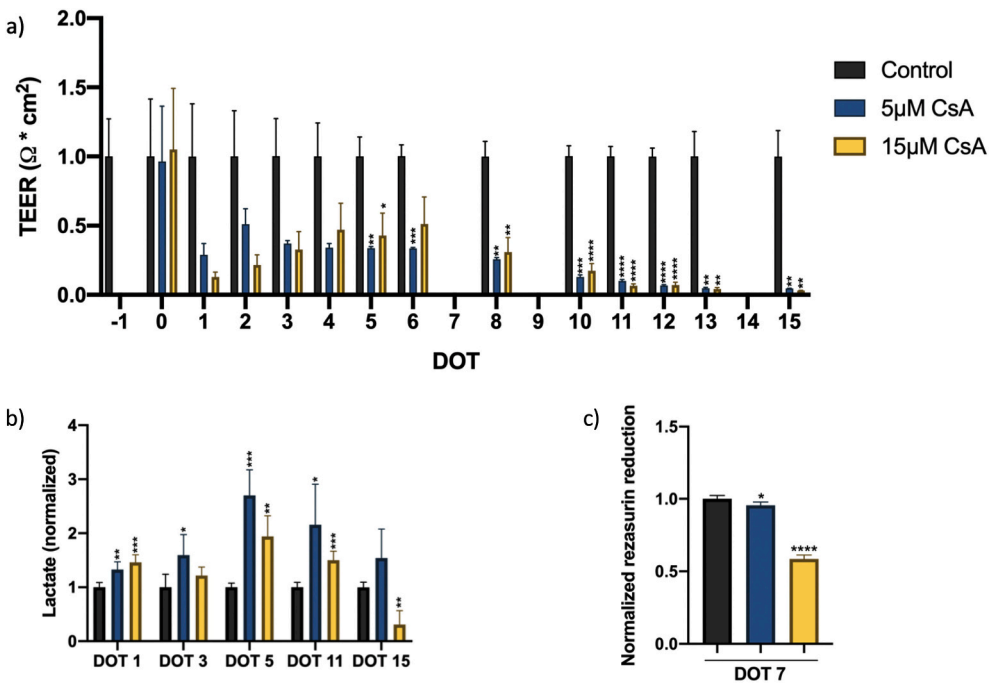


Fig. 3. Repeated dose toxicity assessment. Treatment of BLECs with either 5 μM or 15 μM Cyclosporine A (CsA) were initiated on DOT 0 and renewed every 48 h until DOT 15.
a) Transendothelial Electrical Resistance (TEER) was measured daily except on DOT 7, 9 and 14. Values represent the mean ± SEM of six biological replicates normalized to control condition in the absence of CsA (0.1% DMSO). Statistical significance was determined using repeated measures two-way ANOVA with Dunnett's multiple comparison test (* $p < 0.05$, ** $p < 0.01$, *** $p < 0.001$, **** $p < 0.0001$).
b) Lactate production after 1, 3, 5 or 11 days of BLECs repeated dose treatment with either 5 μM or 15 μM CsA. Lactate was measured in supernatant medium collected 24 h after the last treatment. Values represent the mean ± SD from six biological replicates normalized to the amount of lactate found in supernatant medium of untreated cells (0.1% DMSO) collected on the same DOT. Statistical significance was determined using repeated measures two-way ANOVA with Dunnett's multiple comparison test (* $p < 0.05$, ** $p < 0.01$, *** $p < 0.001$).
c) Cell viability after 7 days of repeated dose treatment with either 5 μM or 15 μM CsA (i.e. at DOT 7). Resazurin assay was conducted 24 h after the last treatment. Values represent the mean ± SD from six biological replicates normalized to resorufin in the absence of CsA (0.1% DMSO). Statistical significance was determined using One-way ANOVA with Dunnett's multiple comparisons test (* $p < 0.05$, *** $p < 0.001$).

over time under 15 μM as reflected by the much lower reduction of resazurin at DOT 7 (*Fig. 3*c) and the lower lactate production compared to control at DOT 15 (*Fig. 3*b). This reduced viability at DOT 15 was confirmed by the reduced number of DAPI-stained nuclei (data not shown). Based on these results, the 15 μM CsA treatment condition at DOT 15 was excluded from targeted RNA sequencing analysis.

3.4. *TempO-Seq transcriptomics analysis of repeated-dose treatment*

Transcriptomics has been a key tool in allowing a better understanding on how the cellular program is altered in response to stress situations (Jennings et al., 2013). In the present study we have used the new, cost-effective technique TempO-Seq to study the effects of repeated-dose treatment on BLECs with CsA (Limonciel et al., 2018; Yeakley et al., 2017). Samples were harvested for targeted RNA sequencing (TempO-Seq) at DOT 0, 1, 3, 5, 11 and 15 and we utilised a probe set identifying 3257 genes which is a combination of a previously selected gene panel (Mav et al., 2018) supplemented with knowledge-based cellular stress response-related genes identified by the experiences of the academic groups in this publication (entire gene set provided in Table S1).

First, we investigated the changes in the transcriptomic profile of BLECs derived from iPSCs over time without treatment. A differential expression analysis was performed for all time points in comparison with DOT 0 (Fig. 4). The amount of differentially expressed genes (DEGs) increases over time suggesting that numerous biological processes are ongoing within the cultures over the two weeks treatment period. Then the effects of repeated-dose CsA treatment on BLECs transcriptional responses has been investigated by comparing the gene expression of treated and untreated condition at the same time point

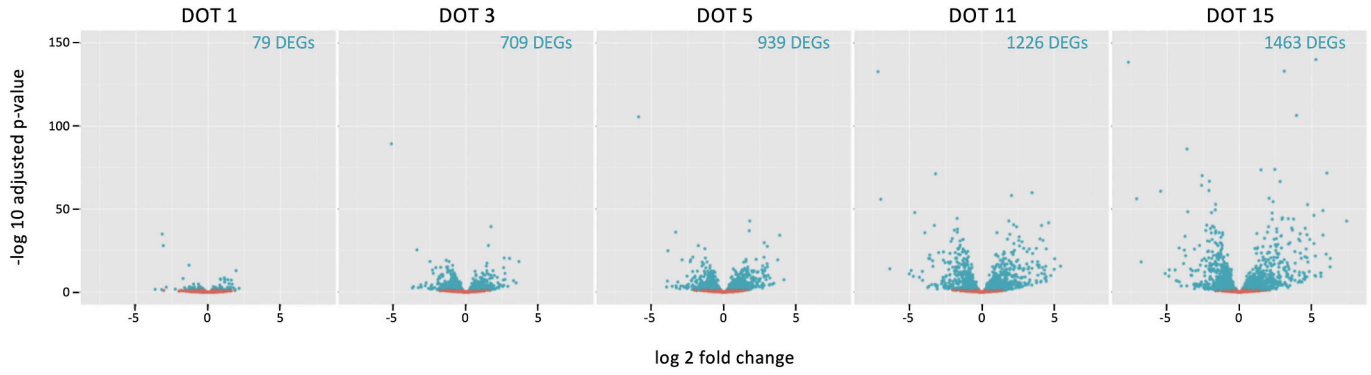


Fig. 4. Volcano plots of BLECs targeted TempO-Seq transcriptomic data over time without CsA treatment.
The averages of gene expression data ($n = 4$) at DOT 1, 3, 5, 11 and 15 were compared using DESeq2 with the averages of gene expression at DOT 0. Blue dots are differentially expressed genes (DEGs) with an adjusted p-value <0.05. The amount of DEGs within these criteria are also given in the top right corner. The DEGs with an adjusted p-value >0.05 are indicated by a red dot. Shrunken log 2-fold changes are shown on the x-axis.

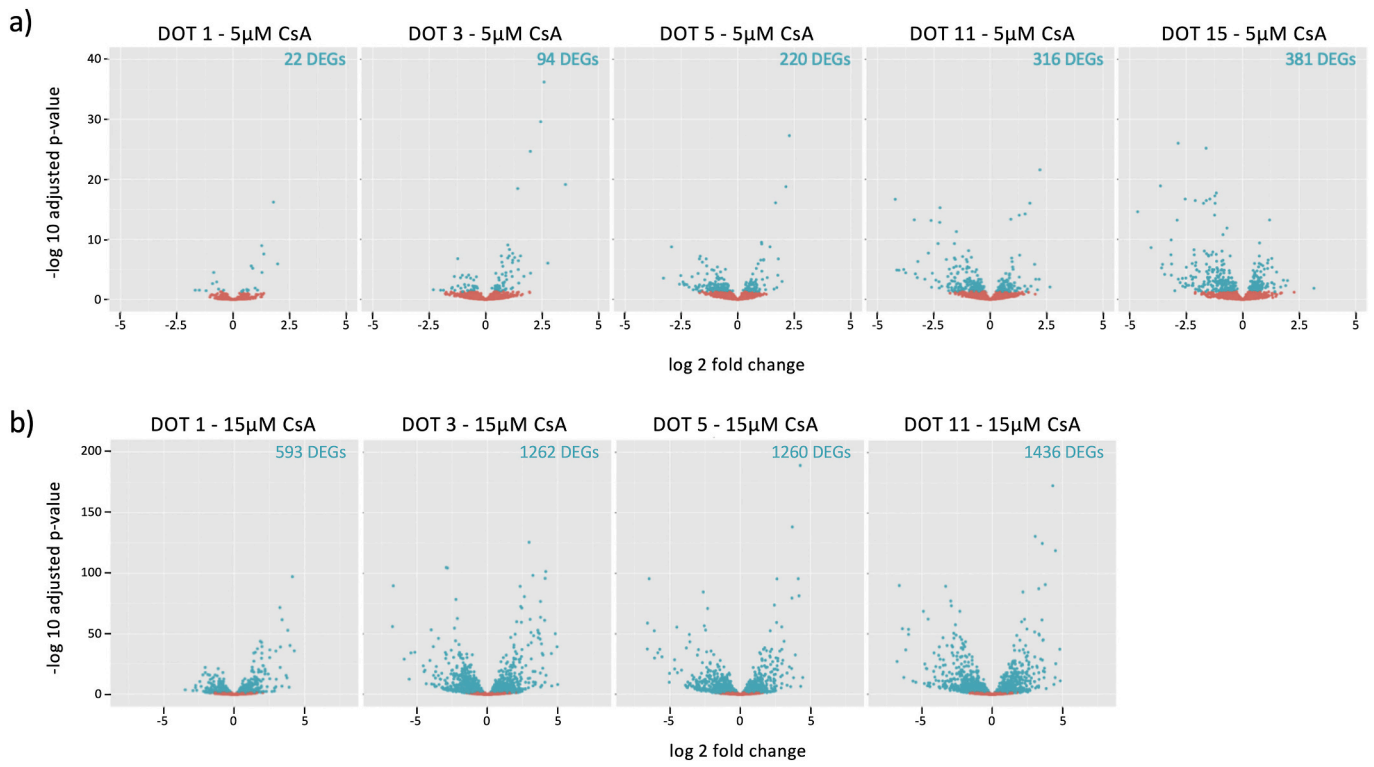


Fig. 5. Volcano plots of BLECs targeted TempO-Seq transcriptomic data with Cyclosporine A (CsA) repeated dose treatment at 5 μM or 15 μM.
a) The averages of gene expression data (n = 4) in BLECs under repeated dose treatment with 5 μM CsA at DOT 1, 3, 5, 11 and 15 were compared with the averages of gene expression in untreated BLECs (0.1% DMSO) at the same DOT.
b) The averages of gene expression data (n = 4) in BLECs under repeated dose treatment with 15 μM CsA at DOT 1, 3, 5, 11 and 15 were compared with the averages of gene expression in untreated BLECs (0.1% DMSO) at the same DOT.
Blue dots are differentially expressed genes (DEGs) with an adjusted *p*-value <0.05. The amount of DEGs within these criteria are also given in the top right corner. The DEGs with an adjusted *p*-value >0.05 are indicated by a red dot. Shrunken log 2-fold changes are shown on the x-axis.

(Fig. 5). The amount of DEGs upon exposure to 5 μM CsA is gradually increasing over time from 22 DEGs at DOT 1 to 316 DEGs at DOT 11 (or 381 DEGs at DOT 15) (*Fig. 5*a). A higher number of genes were found to be differentially expressed upon exposure to 15 μM CsA which was also increasing over time with 593 DEGs at DOT 1 and 1436 DEGs at DOT 11 (*Fig. 5*b). Therefore, both the concentration and the duration of the exposure increased the number of DEGs.

3.5. Stress response pathway analysis using z-scoring

Several transcriptionally regulated pathways have been discovered which could be used to uncover the toxicological responses of specific cell-types to chemicals. Using the data from TempO-Seq analysis, the effects of repeated dose treatment with CsA on some of these pathways has been investigated (Table 1). Pathways with a z-score above 1.96 were considered overrepresented while pathways with a z-score below −1.96 were considered underrepresented. The unfolded protein response pathway ATF4 was overrepresented at all time points for both 5 μM and 15 μM CsA treatment. The z-score was highest at the earliest time point and gradually reduced in both conditions. Over-representation of the oxidative stress response pathway Nrf2 was present in the 15 μM CsA condition at all time points while for the 5 μM CsA

Table 1
Toxicity pathway analysis: z-scores.

Toxicity pathway analysis: z-scores																		
Day	ATF4		XBP1		Nrf2		p53		NFkB		AhR		PPARG		HIF1α		MTF1	
	5 μM	15 μM	5 μM	15 μM	5 μM	15 μM	5 μM	15 μM	5 μM	15 μM	5 μM	15 μM	5 μM	15 μM	5 μM	15 μM	5 μM	15 μM
DOT1	12.4	7.8	-0.3	2.7	1.3	5.3	-0.6	3.2	-0.3	1.4	-0.4	2.2	-0.4	-1.4	-0.3	1.8	-0.3	-0.6
DOT3	12.2	6.1	0.8	3.0	3.4	4.8	-0.5	3.7	1.1	0.6	1.3	1.4	-0.7	-0.5	-0.7	0.6	-0.7	0.3
DOT5	6.4	6.1	2.0	3.0	0.9	4.1	-0.4	3.2	1.8	-0.9	0.8	1.0	-0.2	0.0	-0.2	1.6	-0.1	1.3
DOT11	6.4	3.2	1.3	4.0	0.8	3.2	-1.1	2.6	-0.6	0.1	1.4	1.1	-1.4	0.0	-0.6	0.6	-1.3	-0.1
DOT15	2.6		1.7		0.0		1.1		-1.0		1.5		-0.8		2.2		-1.5	

Z-scores were calculated using the transcriptional expression of annotated genes of treated (5 or 15 μM Cyclosporine A) BLECs after DESeq2 analysis (in comparison with untreated BLECs of the same time point).
Only genes with an adjusted *p*-value <0.05 were included. Pathways with a z-score above 1.96 were considered significantly over-represented while pathways with a z-score below −1.96 were considered significantly under-represented.

condition this was exclusively the case at DOT 3. The p53 pathway was only overrepresented at 15 μM CsA, indicating a clear difference in cellular response between 5 μM and 15 μM CsA. For both AhR and HIF1α a slight overrepresentation (z-score: 2.2) of these pathways was identified at one particular time point. No over-representation of NFκB, PPARG and MTF1 pathways was observed at any of the tested time-point or concentration.

3.6. Top ten differentially expressed genes

To gain further insight into the effects of repeated dose treatment with CsA, we examined the ten most upregulated genes under CsA treatment compared to the controls (Table 2). The gene NMRAL2P appears twice in the list of the top ten most differentially expressed genes at DOT 3 under 15 μM CsA, as this gene was found upregulated by two independent probes to sequence this gene. Several genes appear in the top ten for different time-points (e.g. 8 out of the 10 genes with the highest fold change at DOT 5 under 5 μM CsA treatment are also in the top 10 of at least one other time point with this concentration). Six genes were found in the top ten of the most differentially expressed gene compared to control at different time-point for both CsA concentrations. For example, CHAC1 (ChaC glutathione specific gamma-glutamylcyclotransferase 1) is present in the top ten of almost all 5 μM CsA time points, with exception of DOT 15 and at DOT 1 of 15 μM CsA. Interestingly, ABCG2 (aka BCRP) is present in the top 10 at the latest time points for both concentrations. CsA is known to be a substrate of several efflux transporter expressed in BLECs including ABCG2. Therefore, its increased expression at the cell membrane could reduce the cellular uptake of CsA.

Some of the most upregulated genes at both concentrations of CsA are part of the ATF4 and Nrf2 stress response pathways. Some of the most downregulated genes (Table S3) are also part of the ATF4 (5 μM CsA) and Nrf2 (15 μM CsA) pathways, which supports the findings of our pathway analysis.

4. Discussion

Current safety assessment is moving towards animal free methods, striving for pathway orientated understanding of the molecular changes after exposure to chemicals. The evaluation of compounds toxicity towards the BBB is a crucial component in the assessment of neurotoxicity (Schultz et al., 2015). By restricting their access to the CNS compartment, the BBB prevents numerous potentially neurotoxic agents from reaching toxic concentrations in the brain. However, some chemicals could exert deleterious effects at the BBB, thereby disrupting CNS homeostasis and ultimately resulting in (indirect) neurotoxicity. Indeed, neurological impairment is one of the most frequent adverse reactions to chronic drug treatment and several studies have suggested that some compounds could be toxic towards BBB at concentrations which do not produce any toxic effects on neurons (Hallier-Vanuxeem et al., 2009; Pimentel et al., 2020).

Within the framework of the European Predict-IV (FP7: 2008–2013) project, which aimed to define a strategy for the identification of chronic adverse drug reactions, we demonstrated the possibility to evaluate repeated dose-toxicity of chemicals at the BBB using an animal-derived BBB model (Fabulas-da Costa et al., 2013). However, species-specific differences in the type and expression level of transporters limit the utility of animal models in toxicological studies. Immortalization of human primary BBB endothelial cells have permitted modelling of the human BBB *in vitro*, but limitations such as lack of sufficient barrier properties of these cells have hindered their potential as BBB models. The use of human iPSCs as a renewable source of BLECs for *in vitro* BBB modelling constitute a great opportunity to overcome these shortcomings and since the seminal work of E. Shusta *et al.* in 2012 (Lippmann et al., 2012), several protocols have been published to differentiate iPSC into BLECs (Workman and Svendsen, 2020). The likeliness of these cells to primary human brain microvascular endothelial cells (BMECs) is still debatable. Depending on the phenotypic marker(s) used, the endothelial or epithelial nature of the iPSC-derived BLECs could be questioned (Delsing et al., 2018). Since primary and transformed BMECs exhibit reduced barrier properties once removed from the brain microenvironment and can begin to de-differentiate following prolonged culture periods, this renders the transcriptomic comparison between primary and iPSC derived BLECs quite challenging (Fujimoto et al., 2020). Indeed, the transcriptional expression at the level of the brain vasculature has been reported to be different in arterioles, capillaries and venules (Vanlandewijck et al., 2018). Given the challenge of assessing the differentiation status of the iPSC towards BLECs, the targeted transcriptional data is provided as supplementary material providing in depth information on the culture used.

Variability in the iPSC to BLECs differentiation efficiency depending on the iPSC line used, has already been reported (Patel et al., 2017) and it was then not surprising that differentiation protocol from Qian *et al.* (Qian et al., 2017) had to be adapted to the SBAD3 clone 1 iPSC cell line. Adaptations included changing the seeding density, shortening the culture time in mTeSR and the differentiation time in DeSR2 medium. However, even after these optimizations of the protocol to the iPSC line, striking differences in barrier formation (based on TEER recording) were observed between differentiations, even when these differentiations were performed in parallel with iPSC having the same passage number. Despite that we selected a serum-free, fully defined differentiation medium to reduce variability between differentiations, we had to discard some of the differentiations prepared for this study and only used the ones displaying our minimal requirements (i.e. TEER higher than 25 Ω. cm^2 and functionality of efflux transporters at DOT 0). The observed variability between different differentiations of the same iPSCs line to BLECs with this protocol (Qian et al., 2017) would hamper the use of such model, in particular for regulatory purposes.

Different strategies might be implemented in the future to reduce this variability. First, as the use of Matrigel for cell inserts coating could be a plausible source of variability due to its batch-to-batch variation (Aisenbrey and Murphy, 2020), its substitution by more defined alternatives such as Collagen IV/fibronectin may increase the reproducibility of iPSCs to BLECs differentiation and provide a solution (Qian et al., 2017). Secondly, it has been reported that the iPSC seeding density before the start of the differentiation might influence the TEER of the differentiated BLECs (Wilson et al., 2015). Although we tested different seeding densities of SBAD-3 clone 1 iPSC cell line in the framework of this study, it might be that other iPSC cell lines with different yield or proliferation rate are more suitable for robust differentiations into BLECs. Finally, as co-culturing BLECs with brain pericytes and/or astrocytes has been reported to lead to an increase in TEER and upregulation of BBB associated genes, this might provide a possibility to reduce the variability of iPSCs to BLECs differentiation (Appelt-Menzel et al., 2020; Canfield et al., 2019; Canfield et al., 2017; Heymans et al., 2020).

Since the BLECs resulting from our successful differentiations were able to maintain their BBB characteristics (i.e. TEER higher than 25 Ω. cm^2, claudin-5 expression at cell border, functional expression of efflux transporters) we have used these cultures to investigate the effects of repeated-dose treatment with CsA over a two-week period. The variation in barrier tightness over the two-week period following differentiation is similar to the one recently reported by Neal *et al.* (Neal et al., 2019). This and the increasing amount of DEGs over-time could indicate that the model is undergoing some maturational changes over the 15 days post-differentiation. Therefore, chemically induced transcriptional changes in BLECs should be analysed with caution as the cells are likely to respond differently to the chemical challenge depending on their maturation status. Nevertheless, the comparison of the targeted RNA sequencing using TempO-Seq of BLECs following treatment with CsA to BLECs from the corresponding control group (i.e. untreated BLECs from the same differentiation at the same time point) revealed the time and concentration dependant over-representation of some stress response

Table 2
Top ten most upregulated differentially expressed genes at each time point.

Top 10 upregulated genes									
5μM Cyclosporine A					15μM Cyclosporine A				
Gene	Gene description	log2 FC	padj	Tox-pathway	Gene	Gene description	log2 FC	padj	Tox-pathway
DOT 1					*DOT 1*				
CHAC1	ChaC glutathione specific gamma-glutamylcyclotransferase 1	2.1	1.2E-06	ATF4	G0S2	G0/G1 switch 2	5.8	1.8E-03	
ASNS	asparagine synthetase (glutamine-hydrolyzing)	1.8	6.3E-17	ATF4	INHBE	inhibin subunit beta E	5.6	1.3E-06	
PSAT1	phosphoserine aminotransferase 1	1.4	2.7E-08	ATF4,Nrf2	TRIB3	tribbles pseudokinase 3	5.2	1.3E-268	ATF4
VEGFA	vascular endothelial growth factor A	1.3	3.3E-05		NMRAL2P	NmrA like redox sensor 2, pseudogene	4.6	3.8E-03	
MTHFD2	methylenetetrahydrofolate dehydrogenase (NADP+ dependent) 2	1.3	1.1E-09	ATF4	CHAC1	ChaC glutathione specific gamma-glutamylcyclotransferase 1	4.5	1.4E-36	ATF4
DBNDD2	dysbindin domain containing 2	1.1	2.9E-02		SLC1A4	solute carrier family 1 member 4	4.4	1.9E-07	ATF4
DDIT3	DNA damage inducible transcript 3	1.0	1.3E-02	ATF4	MYOCD	myocardin	4.3	9.3E-03	
TRIB3	tribbles pseudokinase 3	0.9	6.5E-06	ATF4	CSTA	cystatin A	4.3	2.5E-14	
CARS	cysteinyl-tRNA synthetase 1	0.8	2.7E-06	ATF4	ASNS	asparagine synthetase (glutamine-hydrolyzing)	4.2	5.7E-98	ATF4
ATF4	activating transcription factor 4	0.7	2.9E-02	ATF4,Nrf2	ASS1	argininosuccinate synthase 1	4.1	4.1E-41	NFkB
DOT 3					*DOT 3*				
CHAC1	ChaC glutathione specific gamma-glutamylcyclotransferase 1	3.9	7.3E-20	ATF4	NMRAL2P	NmrA like redox sensor 2, pseudogene	7.8	7.7E-09	
SLC7A11	solute carrier family 7 member 11	3.3	9.2E-07	ATF4	GPAT3	glycerol-3-phosphate acyltransferase 3	6.4	1.3E-07	
ASNS	asparagine synthetase (glutamine-hydrolyzing)	2.6	6.2E-37	ATF4	NMRAL2P	NmrA like redox sensor 2, pseudogene	5.8	3.4E-02	
PSAT1	phosphoserine aminotransferase 1	2.5	2.5E-30	ATF4,Nrf2	G0S2	G0/G1 switch 2	5.8	1.0E-03	
VEGFA	vascular endothelial growth factor A	2.2	4.3E-05		CCL4	C-C motif chemokine ligand 4	5.6	6.2E-03	
MTHFD2	methylenetetrahydrofolate dehydrogenase (NADP+ dependent) 2	2.0	2.2E-25	ATF4	INHBE	inhibin subunit beta E	5.5	8.5E-07	
STC2	stanniocalcin 2	1.8	1.5E-04	ATF4	S100A14	S100 calcium binding protein A14	5.4	5.1E-40	
DDIT3	DNA damage inducible transcript 3	1.6	5.7E-08	ATF4	EGFL6	EGF like domain multiple 6	5.3	1.2E-10	
INSIG1	insulin induced gene 1	1.6	1.9E-03	Nrf2	SPP1	secreted phosphoprotein 1	5.1	7.7E-51	NFkB
ASS1	argininosuccinate synthase 1	1.5	1.1E-05		TRIB3	tribbles pseudokinase 3	5.1	3.1E-267	ATF4
DOT 5					*DOT 5*				
LOC284561		3.9	1.9E-02		GPAT3	glycerol-3-phosphate acyltransferase 3	6.4	2.5E-07	
CSTA	cystatin A	2.4	1.1E-02		LOC284561		6.3	4.4E-07	
SLC7A11	solute carrier family 7 member 11	2.4	1.0E-03	ATF4	CSTA	cystatin A	5.4	1.3E-14	
ASNS	asparagine synthetase (glutamine-hydrolyzing)	2.3	5.2E-28	ATF4	CCL4	C-C motif chemokine ligand 4	5.1	1.3E-02	
PSAT1	phosphoserine aminotransferase 1	2.2	1.7E-19	ATF4,Nrf2	GLIS3	GLIS family zinc finger 3	4.6	3.1E-03	
CHAC1	ChaC glutathione specific gamma-glutamylcyclotransferase 1	2.0	9.5E-05	ATF4	TRIB3	tribbles pseudokinase 3	4.3	6.4E-190	ATF4
PTX3	pentraxin 3	1.9	1.8E-07	NFkB	SLC7A11	solute carrier family 7 member 11	4.3	2.0E-14	ATF4
MTHFD2	methylenetetrahydrofolate dehydrogenase (NADP+ dependent) 2	1.7	8.3E-17	ATF4	SAMD9L	sterile alpha motif domain containing 9 like	4.3	1.8E-03	
MYC	MYC proto-oncogene, bHLH transcription factor	1.5	1.8E-09	NFkB	PSAT1	phosphoserine aminotransferase 1	4.3	4.0E-82	ATF4,Nrf2
STC2	stanniocalcin 2	1.4	2.4E-02	ATF4	ASNS	asparagine synthetase (glutamine-hydrolyzing)	4.2	3.1E-96	ATF4
DOT 11					*DOT 11*				
GSC	goosecoid homeobox	3.9	8.7E-03		GPAT3	glycerol-3-phosphate acyltransferase 3	7.1	6.9E-09	
GPAT3	glycerol-3-phosphate acyltransferase 3	3.9	1.9E-02		LAMB3	laminin subunit beta 3	6.3	1.7E-05	
IGF1	insulin like growth factor 1	3.1	2.5E-02	Nrf2	SAMD9L	sterile alpha motif domain containing 9 like	5.7	7.4E-12	
STEAP1	STEAP family member 1	2.8	4.5E-04	Nrf2	SQRDL	sulfide quinone oxidoreductase	5.4	6.3E-04	Nrf2
CSF1R	colony stimulating factor 1 receptor	2.4	4.6E-02		ABCG2	ATP binding cassette subfamily G member 2 (Junior blood group)	5.3	4.3E-26	Nrf2, AhR
TPPP3	tubulin polymerization promoting protein family member 3	2.3	4.4E-04		AFP	alpha fetoprotein	5.2	1.3E-14	NFkB
PSAT1	phosphoserine aminotransferase 1	2.3	2.6E-22		FOSL1	FOS like 1, AP-1 transcription factor subunit	5.2	4.8E-38	p53
CHAC1	ChaC glutathione specific gamma-glutamylcyclotransferase 1	2.2	1.4E-06	ATF4	DOCK2	dedicator of cytokinesis 2	4.7	2.0E-02	
IGF1	insulin like growth factor 1	2.1	6.3E-03	Nrf2	BCL2L13	BCL2 like 13	4.6	1.5E-02	
SLC7A11	solute carrier family 7 member 11	1.8	6.1E-03		UCHL1	ubiquitin C-terminal hydrolase L1	4.6	8.4E-120	
DOT 15									
NRG1	neuregulin 1	4.2	1.4E-02	NFkB					
STAT4	signal transducer and activator of transcription 4	2.3	5.1E-03						
FIGF	vascular endothelial growth factor D	2.2	7.2E-04						
STEAP1	STEAP family member 1	2.0	6.5E-04	ATF4					
ABCG2	ATP binding cassette subfamily G member 2 (Junior blood group)	2.0	3.0E-03	Nrf2, AhR					
AREG	amphiregulin	2.0	8.6E-03						
IFNGR1	interferon gamma receptor 1	1.7	5.0E-02						
CYP26A1	cytochrome P450 family 26 subfamily A member 1	1.7	2.8E-05						
FOLH1	folate hydrolase 1	1.5	1.2E-02						
MYBL1	MYB proto-oncogene like 1	1.4	1.6E-03						

Color code
Genes in blue: reappearing in 5 μM group
Genes in yellow: reappearing in 15 μM group
Genes in green: reappearing in 5 μM and 15 μM group

Gene expression in BLECs treated with either 5 or 15 μM Cyclosporine A (CsA) was compared to gene expression in untreated BLECs from the same time point.

For each time-point, the ten most highly upregulated genes are displayed with log 2-fold change and an adjusted p-value <0.05. Genes in blue reappear over the different time points of the 5 μM CsA treated BLECs. Genes in yellow reappear over the different time points of the 15 μM CsA treated BLECs. Genes in green appear in both the 5 μM and 15 μM CsA treated BLECs. Duplicated genes within one specific condition are sequenced using different probes.

pathway (based on z-scoring). For both concentrations, 5 μM and 15 μM CsA, a significant increase in z-score for the unfolded protein response transcription factor ATF4 pathway was observed which was also reported in human renal epithelial cells (RPTEC/TERT1) and human liver cells (HepaRG) at 15 μM CsA (Limonciel et al., 2018; Wilmes et al., 2013). Similarly, the unfolded protein response XBP1 branch and oxidative stress response pathway Nrf2 were found activated under repeated dose treatment with CsA at 15 μM which was also the case in RPTEC/TERT1 cells (Wilmes et al., 2013).

The activation of the p53 pathway, involved in cell cycle arrest and apoptosis, is observed under repeated-dose treatment with 15 μM CsA from DOT 1 to DOT 11. This might explain the cell loss at this concentration already indicated by the decreased reduction of resazurin at DOT 7, reduced viability at DOT 15 and the decreased number of nuclei at DOT 15. Although, the z-scores for ATF4 are the highest at the earliest time points for both 5 and 15 μM CsA, the lower z-scores at later time points do not imply that the fold change of the genes within this pathway are decreasing over time. This is also reflecting additional changes in other cellular processes, indicated by the higher amount of DEGs at the later time points. Furthermore, the lower z-score under 15 μM CsA compared to 5 μM CsA might also reflect additional cellular changes due to the severity of the toxicological insult at this concentration.

The adaptation of an iPSC derived model for repeated dose treatment with the used protocol still remains challenging as illustrated by the differentiation-to-differentiation variability and ongoing transcriptional changes after differentiation. The implementation of cell sorting strategies to increase BLECs homogeneity, completely chemically defined cell culture products and effective methods for the cryopreservation of these differentiated cells would improve the reproducibility and scalability of BLECs for toxicological use (Praça et al., 2019; Qian et al., 2017; Wilson et al., 2016). Despite this variability and ongoing maturational changes over the two weeks treatment period, the combination of targeted TempO-Seq transcriptomics and transcriptomic pathway analysis evidenced the dose and time specific activation of ATF4, XBP1, NRF2 and p53 pathways by CsA in BLECs. Taken as a whole, the results of this study demonstrate that iPSCs derived BBB models hold a great potential to study the effects of repeated dose treatment.

Declaration of Competing Interest

The authors declare no conflict of interest. The funders had no role in the design of the study; in the collection, analyses, or interpretation of data; in the writing of the manuscript, or in the decision to publish the results.

Acknowledgements

We would like to thank Anja Wilmes (Division of Molecular and Computational Toxicology, Amsterdam Institute for Molecules, Medicines and Systems, Vrije Universiteit Amsterdam, The Netherlands) and Marie-Gabrielle Zurich (Department of Physiology, University of Lausanne, Switzerland) for their feedback and suggestions.

The work was funded by the Marie Sklodowska-Curie Action-Innovative Training Network project in3, under grant no. 721975 (fellowship to Sara Wellens, Vidya Chandrasekaran and Pranika Singh).

Fabien Gosselet and Rodrigo Azevedo Loiola were partially supported by the Euronanomed 8th Joint Call-MAGBBRIS collaborative project by grants from the French national agency (ANR-ANR-17-ENM3-0005-01).

Appendix B. Supplementary data

Supplemental-Files-4 - This folder contains the R-script in jupyter notebook format (TempO-Seq-analysis-Workflow24March2020.ipynb) together with the raw data (raw_data-UART02-SBAD3U.csv) and metadata (metadata-UART02-SBAD3U.csv) used for the analysis.

References

Aisenbrey, E.A., Murphy, W.L., 2020. Synthetic alternatives to Matrigel. Nature Reviews Materials 5, 539–551. https://doi.org/10.1038/s41578-020-0199-8.

Alqawi, O., Bates, S., Georges, E., 2004. Arginine482 to threonine mutation in the breast cancer resistance protein ABCG2 inhibits rhodamine 123 transport while increasing binding. Biochem. J. 382, 711–716. https://doi.org/10.1042/BJ20040355.

Appelt-Menzel, A., Cubukova, A., Günther, K., Edenhofer, F., Piontek, J., Krause, G., Stüber, T., Walles, H., Neuhaus, W., Metzger, M., 2017. Establishment of a human blood-brain barrier co-culture model mimicking the neurovascular unit using induced pluri- and multipotent stem cells. Stem Cell Rep. 8, 894–906. https://doi.org/10.1016/j.stemcr.2017.02.021.

Appelt-Menzel, A., Oerter, S., Mathew, S., Haferkamp, U., Hartmann, C., Jung, M., Neuhaus, W., Pless, O., 2020. Human iPSC-derived blood-brain barrier models: valuable tools for preclinical drug discovery and development? Curr. Protoc. Stem Cell Biol. 55, e122 https://doi.org/10.1002/cpsc.122.

Bal-Price, A., Pistollato, F., Sachana, M., Bopp, S.K., Munn, S., Worth, A., 2018. Strategies to improve the regulatory assessment of developmental neurotoxicity (DNT) using in vitro methods. Toxicol. Appl. Pharmacol. 354, 7–18. https://doi.org/10.1016/j.taap.2018.02.008.

Boyer-Di Ponio, J., El-Ayoubi, F., Glacial, F., Ganeshamoorthy, K., Driancourt, C., Godet, M., Perrière, N., Guillevic, O., Olivier Couraud, P., Uzan, G., 2014. Instruction of circulating endothelial progenitors in vitro towards specialized blood-brain barrier and arterial phenotypes. PLoS One 9. https://doi.org/10.1371/journal.pone.0084179.

Canfield, S.G., Stebbins, M.J., Morales, B.S., Asai, S.W., Vatine, G.D., Svendsen, C.N., Palecek, S.P., Shusta, E.V., 2017. An isogenic blood–brain barrier model comprising brain endothelial cells, astrocytes, and neurons derived from human induced pluripotent stem cells. J. Neurochem. 140, 874–888. https://doi.org/10.1111/jnc.13923.

Canfield, S.G., Stebbins, M.J., Faubion, M.G., Gastfriend, B.D., Palecek, S.P., Shusta, E.V., 2019. An isogenic neurovascular unit model comprised of human induced pluripotent stem cell-derived brain microvascular endothelial cells, pericytes, astrocytes, and neurons. Fluids Barriers CNS 16, 1–12. https://doi.org/10.1186/s12987-019-0145-6.

Cecchelli, R., Aday, S., Sevin, E., Almeida, C., Culot, M., Dehouck, L., Coisne, C., Engelhardt, B., Dehouck, M.P., Ferreira, L., 2014. A stable and reproducible human blood-brain barrier model derived from hematopoietic stem cells. PLoS One 9. https://doi.org/10.1371/journal.pone.0099733.

Delsing, L., Dönnes, P., Sánchez, J., Clausen, M., Voulgaris, D., Falk, A., Herland, A., Brolén, G., Zetterberg, H., Hicks, R., Synnergren, J., 2018. Barrier properties and transcriptome expression in human iPSC-derived models of the blood–brain barrier. Stem Cells 36, 1816–1827. https://doi.org/10.1002/stem.2908.

Eigenmann, D.E., Xue, G., Kim, K.S., Moses, A.V., Hamburger, M., Oufir, M., 2013. Comparative study of four immortalized human brain capillary endothelial cell lines, hCMEC/D3, hBMEC, TY10, and BB19, and optimization of culture conditions, for an in vitro blood-brain barrier model for drug permeability studies. Fluids Barriers CNS 10. https://doi.org/10.1186/2045-8118-10-33.

Fabulas-da Costa, A., Aijjou, R., Hachani, J., Landry, C., Cecchelli, R., Culot, M., 2013. In vitro blood-brain barrier model adapted to repeated-dose toxicological screening. Toxicol. in Vitro 27, 1944–1953. https://doi.org/10.1016/j.tiv.2013.06.026.

Fritsche, E., 2017. OECD/EFSA workshop on developmental neurotoxicity (DNT): the use of non-animal test methods for regulatory purposes. ALTEX 34, 311–315. https://doi.org/10.14573/altex.1701171s.

Fujimoto, T., Morofuji, Y., Nakagawa, S., Kovac, A., Horie, N., Izumo, T., Niwa, M., Matsuo, T., Banks, W.A., 2020. Comparison of the rate of dedifferentiation with increasing passages among cell sources for an in vitro model of the blood–brain barrier. J. Neural Transm. 127, 1117–1124. https://doi.org/10.1007/s00702-020-02202-1.

Hallier-Vanuxeem, D., Prieto, P., Culot, M., Diallo, H., Landry, C., Tähti, H., Cecchelli, R., 2009. New strategy for alerting central nervous system toxicity: integration of blood-brain barrier toxicity and permeability in neurotoxicity assessment. Toxicol. in Vitro 23, 447–453. https://doi.org/10.1016/j.tiv.2008.12.011.

Hauben, M., 1996. Cyclosporine neurotoxicity. Pharmacotherapy 16, 576–583. https://doi.org/10.1002/j.1875-9114.1996.tb03639.x.

Heymans, M., Figueiredo, R., Dehouck, L., Francisco, D., Sano, Y., Shimizu, F., Kanda, T., Bruggmann, R., Engelhardt, B., Winter, P., Gosselet, F., Culot, M., 2020. Contribution of brain pericytes in blood-brain barrier formation and maintenance: a transcriptomic study of cocultured human endothelial cells derived from hematopoietic stem cells. Fluids Barriers CNS 17, 1–28. https://doi.org/10.1186/s12987-020-00208-1.

Hollmann, E.K., Bailey, A.K., Potharazu, A.V., Neely, M.D., Bowman, A.B., Lippmann, E. S., 2017. Accelerated differentiation of human induced pluripotent stem cells to blood–brain barrier endothelial cells. Fluids Barriers CNS 14, 9. https://doi.org/10.1186/s12987-017-0059-0.

Jennings, P., Koppelstaetter, C., Aydin, S., Abberger, T., Wolf, A.M., Mayer, G., Pfaller, W., 2007. Cyclosporine A induces senescence in renal tubular epithelial cells. Am. J. Physiol. Ren. Physiol. 293, 831–838. https://doi.org/10.1152/ajprenal.00005.2007.

Jennings, P., Limonciel, A., Felice, L., Leonard, M.O., 2013. An overview of transcriptional regulation in response to toxicological insult. Arch. Toxicol. 87, 49–72. https://doi.org/10.1007/s00204-012-0919-y.

Kutmon, M., van Iersel, M.P., Bohler, A., Kelder, T., Nunes, N., Pico, A.R., Evelo, C.T., 2015. PathVisio 3: an extendable pathway analysis toolbox. PLoS Comput. Biol. 11, 1–13. https://doi.org/10.1371/journal.pcbi.1004085.

Li, H., Durbin, R., 2009. Fast and accurate short read alignment with burrows-wheeler transform. Bioinformatics 25, 1754–1760. https://doi.org/10.1093/bioinformatics/btp324.

Limonciel, A., Aschauer, L., Wilmes, A., Prajczer, S., Leonard, M.O., Pfaller, W., Jennings, P., 2011. Lactate is an ideal non-invasive marker for evaluating temporal alterations in cell stress and toxicity in repeat dose testing regimes. Toxicol. in Vitro 25, 1855–1862. https://doi.org/10.1016/j.tiv.2011.05.018.

Limonciel, A., Moenks, K., Stanzel, S., Truisi, G.L., Parmentier, C., Aschauer, L., Wilmes, A., Richert, L., Hewitt, P., Mueller, S.O., Lukas, A., Kopp-Schneider, A., Leonard, M.O., Jennings, P., 2015. Transcriptomics hit the target: monitoring of ligand-activated and stress response pathways for chemical testing. Toxicol. in Vitro 30, 7–18. https://doi.org/10.1016/j.tiv.2014.12.011.

Limonciel, A., Ates, G., Carta, G., Wilmes, A., Watzele, M., Shepard, P.J., VanSteenhouse, H.C., Seligmann, B., Yeakley, J.M., van de Water, B., Vinken, M., Jennings, P., 2018. Comparison of base-line and chemical-induced transcriptomic responses in HepaRG and RPTEC/TERT1 cells using TempO-Seq. Arch. Toxicol. 92, 2517–2531. https://doi.org/10.1007/s00204-018-2256-2.

Lippmann, E.S., Azarin, S.M., Kay, J.E., Nessler, R.A., Wilson, H.K., Al-Ahmad, A., Palecek, S.P., Shusta, E.V., 2012. Derivation of blood-brain barrier endothelial cells from human pluripotent stem cells. Nat. Biotechnol. 30, 783–791. https://doi.org/10.1038/nbt.2247.

Lippmann, E.S., Al-Ahmad, A., Palecek, S.P., Shusta, E.V., 2013. Modeling the blood–brain barrier using stem cell sources. Fluids Barriers CNS 10, 2. https://doi.org/10.1186/2045-8118-10-2.

Lippmann, E.S., Al-Ahmad, A., Azarin, S.M., Palecek, S.P., Shusta, E.V., 2014. A retinoic acid-enhanced, multicellular human blood-brain barrier model derived from stem cell sources. Sci. Rep. 4, 4160. https://doi.org/10.1038/srep04160.

Logan, S., Arzua, T., Canfield, S.G., Seminary, E.R., Sison, S.L., Ebert, A.D., Bai, X., 2019. Studying human neurological disorders using induced pluripotent stem cells: from 2D monolayer to 3D organoid and blood brain barrier models. Compr. Physiol. 9, 565–611. https://doi.org/10.1002/cphy.c180025.

Love, M.I., Huber, W., Anders, S., 2014. Moderated estimation of fold change and dispersion for RNA-seq data with DESeq2. Genome Biol. 15, 550. https://doi.org/10.1186/s13059-014-0550-8.

Mav, D., Shah, R.R., Howard, B.E., Auerbach, S.S., Bushel, P.R., Collins, J.B., Gerhold, D. L., Judson, R.S., Karmaus, A.L., Maull, E.A., Mendrick, D.L., Merrick, B.A., Sipes, N. S., Svoboda, D., Paules, R.S., 2018. A hybrid gene selection approach to create the S1500+ targeted gene sets for use in high-throughput transcriptomics. PLoS One 13, 1–19. https://doi.org/10.1371/journal.pone.0191105.

Neal, E.H., Marinelli, N.A., Shi, Y., McClatchey, P.M., Balotin, K.M., Gullett, D.R., Hagerla, K.A., Bowman, A.B., Ess, K.C., Wikswo, J.P., Lippmann, E.S., 2019. A simplified, fully defined differentiation scheme for producing blood-brain barrier endothelial cells from human iPSCs. Stem Cell Rep. 12, 1380–1388. https://doi.org/10.1016/j.stemcr.2019.05.008.

Obermeier, B., Daneman, R., Ransohoff, R.M., 2013. Development, maintenance and disruption of the blood-brain-barrier. Nat. Med. 19, 1584–1596. https://doi.org/10.1038/nm.3407.Development.

Özvegy, C., Varadi, A., Sarkadi, B., 2002. Characterization of drug transport, ATP hydrolysis, and nucleotide trapping by the human ABCG2 multidrug transporter. Modulation of substrate specificity by a point mutation. J. Biol. Chem. 277, 47980–47990. https://doi.org/10.1074/jbc.M207857200.

Patel, R., Page, S., Al-Ahmad, A.J., 2017. Isogenic blood–brain barrier models based on patient-derived stem cells display inter-individual differences in cell maturation and functionality. J. Neurochem. 142, 74–88. https://doi.org/10.1111/jnc.14040.

Pimentel, E., Sivalingam, K., Doke, M., Samikkannu, T., 2020. Effects of drugs of abuse on the blood-brain barrier: a brief overview. Front. Neurosci. 14, 1–9. https://doi.org/10.3389/fnins.2020.00513.

Praça, C., Rosa, S.C., Sevin, E., Cecchelli, R., Dehouck, M.P., Ferreira, L.S., 2019. Derivation of brain capillary-like endothelial cells from human pluripotent stem cell-derived endothelial progenitor cells. Stem Cell Rep. 13, 599–611. https://doi.org/10.1016/j.stemcr.2019.08.002.

Qian, T., Maguire, S.E., Canfield, S.G., Bao, X., Olson, W.R., Shusta, E.V., Palecek, S.P., 2017. Directed differentiation of human pluripotent stem cells to blood-brain barrier endothelial cells. Sci. Adv. 3, e1701679 https://doi.org/10.1126/sciadv.1701679.

Rauch, C., Feifel, E., Kern, G., Murphy, C., Meier, F., Parson, W., Beilmann, M., Jennings, P., Gstraunthaler, G., Wilmes, A., 2018. Differentiation of human iPSCs into functional podocytes. PLoS One 13. https://doi.org/10.1371/journal.pone.0203869.

Schultz, L., Zurich, M.G., Culot, M., da Costa, A., Landry, C., Bellwon, P., Kristl, T., Hörmann, K., Ruzek, S., Aiche, S., Reinert, K., Bielow, C., Gosselet, F., Cecchelli, R., Huber, C.G., Schroeder, O.H.U., Gramowski-Voss, A., Weiss, D.G., Bal-Price, A., 2015. Evaluation of drug-induced neurotoxicity based on metabolomics, proteomics and electrical activity measurements in complementary CNS in vitro models. Toxicol. in Vitro 30, 138–165. https://doi.org/10.1016/j.tiv.2015.05.016.

Sevin, E., Dehouck, L., Versele, R., Culot, M., Gosselet, F., 2019. A miniaturized pump out method for characterizing molecule interaction with ABC transporters. Int. J. Mol. Sci. 20 https://doi.org/10.3390/ijms20225529.

Sirenko, O., Parham, F., Dea, S., Sodhi, N., Biesmans, S., Mora-Castilla, S., Ryan, K., Behl, M., Chandy, G., Crittenden, C., Vargas-Hurlston, S., Guicherit, O., Gordon, R., Zanella, F., Carromeu, C., 2019. Functional and mechanistic neurotoxicity profiling using human iPSC-derived neural 3D cultures. Toxicol. Sci. 167, 249–257. https://doi.org/10.1093/toxsci/kfy218.

Vanlandewijck, M., He, L., Mäe, M.A., Andrae, J., Ando, K., Del Gaudio, F., Nahar, K., Lebouvier, T., Laviña, B., Gouveia, L., Sun, Y., Raschperger, E., Räsänen, M., Zarb, Y., Mochizuki, N., Keller, A., Lendahl, U., Betsholtz, C., 2018. A molecular atlas of cell types and zonation in the brain vasculature. Nature 554, 475–480. https://doi.org/10.1038/nature25739.

Weksler, B.B., Subileau, E.A., Perrière, N., Charneau, P., Holloway, K., Leveque, M., Tricoire-Leignel, H., Nicotra, A., Bourdoulous, S., Turowski, P., Male, D.K., Roux, F., Greenwood, J., Romero, I.A., Couraud, P.O., 2005. Blood-brain barrier-specific properties of a human adult brain endothelial cell line. FASEB J. 19, 1872–1874. https://doi.org/10.1096/fj.04-3458fje.

Wilmes, A., Crean, D., Aydin, S., Pfaller, W., Jennings, P., Leonard, M.O., 2011. Identification and dissection of the Nrf2 mediated oxidative stress pathway in human renal proximal tubule toxicity. Toxicol. in Vitro 25, 613–622. https://doi.org/10.1016/j.tiv.2010.12.009.

Wilmes, A., Limonciel, A., Aschauer, L., Moenks, K., Bielow, C., Leonard, M.O., Hamon, J., Carpi, D., Ruzek, S., Handler, A., Schmal, O., Herrgen, K., Bellwon, P., Burek, C., Truisi, G.L., Hewitt, P., Di Consiglio, E., Testai, E., Blaauboer, B.J., Guillou, C., Huber, C.G., Lukas, A., Pfaller, W., Mueller, S.O., Bois, F.Y., Dekant, W., Jennings, P., 2013. Application of integrated transcriptomic, proteomic and metabolomic profiling for the delineation of mechanisms of drug induced cell stress. J. Proteome 79, 180–194. https://doi.org/10.1016/j.jprot.2012.11.022.

Wilson, H.K., Canfield, S.G., Hjortness, M.K., Palecek, S.P., Shusta, E.V., 2015. Exploring the effects of cell seeding density on the differentiation of human pluripotent stem cells to brain microvascular endothelial cells. Fluids Barriers CNS 12, 13. https://doi.org/10.1186/s12987-015-0007-9.

Wilson, H.K., Faubion, M.G., Hjortness, M.K., Palecek, S.P., Shusta, E.V., 2016. Cryopreservation of brain endothelial cells derived from human induced pluripotent stem cells is enhanced by rho-associated coiled coil-containing kinase inhibition. Tissue Eng. - C Methods 22, 1085–1094. https://doi.org/10.1089/ten.tec.2016.0345.

Workman, M.J., Svendsen, C.N., 2020. Recent advances in human iPSC-derived models of the blood-brain barrier. Fluids Barriers CNS 17, 1–10. https://doi.org/10.1186/s12987-020-00191-7.

Wu, Q., Wang, X., Nepovimova, E., Wang, Y., Yang, H., Kuca, K., 2018. Mechanism of cyclosporine A nephrotoxicity: oxidative stress, autophagy, and signalings. Food Chem. Toxicol. 118, 889–907. https://doi.org/10.1016/j.fct.2018.06.054.

Yeakley, J.M., Shepard, P.J., Goyena, D.E., Vansteenhouse, H.C., McComb, J.D., Seligmann, B.E., 2017. A Trichostatin a expression signature identified by TempO-Seq targeted whole transcriptome profiling. PLoS One 12. https://doi.org/10.1371/journal.pone.0178302.